Feedback Control of Freeway Traffic Flow via Time-Gap Manipulation of ACC-Equipped Vehicles: A PDE-Based Approach

Nikolaos Bekiaris-Liberis * **Argiris Delis** **

* *Departments of Electrical & Computer Engineering and Production Engineering & Management, Technical University of Crete, Chania, Greece, 73100 (e-mail: bekiaris-liberis@ece.tuc.gr).*
** *Department of Production Engineering & Management, Technical University of Crete, Chania, Greece, 73100 (e-mail: adelis@science.tuc.gr).*

Abstract: We develop a control design for stabilization of traffic flow in congested regime, based on an Aw-Rascle-Zhang-type (ARZ-type) Partial Differential Equation (PDE) model, for traffic consisting of both ACC-equipped (Adaptive Cruise Control-equipped) and manual vehicles. The control input is the value of the time-gap setting of ACC-equipped and connected vehicles, which gives rise to a problem of control of a 2×2 nonlinear system of first-order hyperbolic PDEs with in-domain actuation. The feedback law is designed in order to stabilize the linearized system, around a uniform, congested equilibrium profile. Stability of the closed-loop system under the developed control law is shown constructing a Lyapunov functional. The performance improvement of the closed-loop system under the proposed strategy is illustrated in simulation, also employing four different metrics, which quantify the performance in terms of fuel consumption, total travel time, and comfort.

1. INTRODUCTION

Although traffic congestion may be unavoidable nowadays, due to the continuous increase in the number of vehicles and in the traffic demand, some of its ramifications may be alleviated employing real-time traffic control strategies Chen et al. (2001). Among other reasons, certain traffic flow instability phenomena, such as, for example, stop-and-go waves, are some of the causes of traffic congestion's negative consequences on fuel consumption, total travel time, drivers' comfort, and safety Treiber & Kesting (2013). One promising avenue to traffic flow stabilization is the development of control design tools that exploit the capabilities of automated and connected vehicles Diakaki et al. (2015), while retaining the distributed nature of traffic flow dynamics. It is the aim of this paper to develop a feedback law for traffic flow stabilization utilizing a PDE traffic flow model and exploiting the capabilities of ACC-equipped and connected vehicles.

Since second-order, PDE traffic flow models (i.e., systems that incorporate two PDE states, one for traffic density and one for traffic speed) constitute realistic descriptions of the traffic dynamics, capturing important phenomena, such as, for example, stop-and-go traffic, capacity drop, etc. Delis et al. (2015), Fan et al. (2014), Ngoduy (2013) boundary control designs are recently developed for such systems Belletti et al. (2015), Karafyllis et al. (2018), Yu & Krstic (2019), Zhang & Prieur (2017a), Zhang & Prieur (2017b) some of which are based on techniques originally developed for control of systems of hyperbolic PDEs, such as, for example, Bastin & Coron (2016), Herty & Yong (2016), Lamare & Bekiaris-Liberis (2015), Zhang & Prieur (2017a), Vazquez & Krstic (2014). Even though simpler, first-order traffic flow models, in conservation law or Hamilton-Jacobi PDE formulation, are also important for modeling purposes. For this reason, PDE-based control design techniques exist for this class of systems as well Bekiaris-Liberis & Bayen (2014), Blandin et al. (2017), Claudel & Bayen (2010), Delle Monache et al. (2017), Goatin et al. (2016), Li et al. (1995).

While most of the above PDE-based traffic control techniques rely on traditional implementation means such as, ramp metering and variable speed limits, more rare are PDE-based, traffic flow control methodologies that exploit connected and automated vehicles capabilities. In particular, Swaroop & Rajagopal (1999), Yi & Horowitz (2006) develop control designs via in-domain manipulation of acceleration of ACC-equipped vehicles, considering traffic with only automated vehicles, and Piacentini et al. (2018), Yu et al. (2018) develop control designs via speed manipulation of an autonomous vehicle. Furthermore, although in microscopic simulation it is reported that it may be beneficial for traffic flow, to appropriately manipulate in real time the ACC settings of vehicles already equipped with an ACC feature Kesting et al. (2008), Schakel & van Arem (2014), Spiliopoulou et al. (2018), the problem of systematic feedback control design via time-gap manipulation hasn't, heretofore, been tackled from a PDE viewpoint.

In this work, we design a feedback control strategy for stabilization of traffic flow in congested regime, manipulating the time-gap setting of vehicles equipped with ACC and utilizing a control-oriented, ARZ-type model with ACC (which is shown to possess certain important traffic flow-theoretic properties). The control strategy is developed for the linearized system around a uniform, congested equilibrium profile, which is proved to be open-loop unstable. Due to the presence (on average) of a certain penetration rate of ACC-equipped vehicles in a given freeway stretch, the traffic flow control problem is recast to the problem of stabilization of a 2×2 linear system of first-order, heterodirectional hyperbolic PDEs with in-domain actuation. The closed-loop system under the proposed controller is shown to be exponentially stable (in C^1 norm), constructing a Lyapunov functional. The benefits in traffic flow of employing the proposed strategy are illustrated in simulation, also including the quantification of the performance improvement in terms of various indices, measuring total travel time, fuel consumption, and comfort level.

Notation: For $u \in C[0,D]$ we denote $\|u\|_C = \max_{x\in[0,D]} |u(x)|$ and for $u \in C^1[0,D]$ we define $\|u\|_{C^1} = \|u\|_C + \|u'\|_C$.

2. ARZ-TYPE MODEL WITH ACC IN CONGESTED REGIME

2.1 Description of the model

We consider the following system

$$\rho_t(x,t) = -\rho_x(x,t)v(x,t) - \rho(x,t)v_x(x,t) \tag{1}$$

$$v_t(x,t) = -\left(v(x,t) + \rho(x,t)\frac{\partial V_{\mathrm{mix}}(\rho(x,t),h_{\mathrm{acc}}(x,t))}{\partial\rho}\right) \times v_x(x,t) + \frac{V_{\mathrm{mix}}(\rho(x,t),h_{\mathrm{acc}}(x,t)) - v(x,t)}{\tau_{\mathrm{mix}}} \tag{2}$$

$$q_{\mathrm{in}} = \rho(0,t)v(0,t) \tag{3}$$

$$v_t(D,t) = \frac{V_{\mathrm{mix}}(\rho(D,t),h_{\mathrm{acc}}(D,t)) - v(D,t)}{\tau_{\mathrm{mix}}}, \tag{4}$$

where

$$V_{\mathrm{mix}}(\rho,h_{\mathrm{acc}}) = \tau_{\mathrm{mix}}\left(\frac{\alpha}{\tau_{\mathrm{acc}}}V_{\mathrm{acc}}(\rho,h_{\mathrm{acc}}) + \frac{1-\alpha}{\tau_{\mathrm{m}}}V_{\mathrm{m}}(\rho)\right) \tag{5}$$

$$V_{\mathrm{acc}}(\rho,h_{\mathrm{acc}}) = \frac{1}{h_{\mathrm{acc}}}\left(\frac{1}{\rho} - L\right), \quad \rho_{\min} < \rho < \frac{1}{L} \tag{6}$$

$$V_{\mathrm{m}}(\rho) = \frac{1}{h_{\mathrm{m}}}\left(\frac{1}{\rho} - L\right), \quad \rho_{\min} < \rho < \frac{1}{L} \tag{7}$$

$$\tau_{\mathrm{mix}} = \frac{1}{\frac{\alpha}{\tau_{\mathrm{acc}}} + \frac{1-\alpha}{\tau_{\mathrm{m}}}}, \tag{8}$$

ρ is traffic density, $0 < v \le v_{\mathrm{f}}$ is traffic speed, with v_f being some maximum achievable speed (or, free-flow speed), $D > 0$ is length of a given freeway stretch, $L > 0$ is average effective length of each vehicle, $\alpha \in [0,1]$ is the percentage of ACC-equipped vehicles with respect to total vehicles, $\rho_{\min} > 0$ is the lowest value for density for which the model is accurate (see Section 2.2), $t \ge 0$ is time, $x \in [0,D]$ is spatial variable, $q_{\mathrm{in}} > 0$ is a constant external inflow, τ_{acc}, $\tau_{\mathrm{m}} > 0$ are the time constants of the ACC-equipped and manual vehicles, respectively, $h_{\mathrm{m}} > 0$ is the time-gap of manual vehicles, and $h_{\mathrm{acc}} > 0$ is the time-gap of ACC-equipped vehicles, which is the control input.

2.2 Traffic flow-oriented properties of the model

The motivation for model (1)–(4) is the following. First, note that equation (1) is the conservation-of-vehicles equation, as $q = \rho v$ is the traffic flow. Equation (2) is the speed equation, which is inspired by the speed dynamics of the ARZ model Zhang (2002). In fact, the ARZ model may be viewed as both a model of traffic flow dynamics for traffic with only manual vehicles Zhang (2002) as well as a model for traffic flow dynamics with only ACC-equipped vehicles Swaroop & Rajagopal (1999) (Section 3.2). In particular, for fixed time-gaps of ACC-equipped (and manual) vehicles, when $\alpha = 1$ (only ACC-equipped vehicles exist) or $\alpha = 0$ (only manual vehicles exist) the model reduces to the ARZ model with fundamental diagram given by (6) or (7) (which corresponds to the so-called constant time-gap policy, see, e.g., Bose & Ioannou (2003), Swaroop & Rajagopal (1999), Yi & Horowitz (2006)), respectively. However, to account for the case of mixed traffic, i.e., when both manual and ACC-equipped vehicles are present, we define a new equilibrium (fundamental diagram) relation for speed as in (5), which is also written as

$$V_{\mathrm{mix}}(\rho,h_{\mathrm{acc}}) = \frac{1}{h_{\mathrm{mix}}(h_{\mathrm{acc}})}\left(\frac{1}{\rho} - L\right), \tag{9}$$

where the effective (or, mixed) time-gap is defined as

$$h_{\mathrm{mix}}(h_{\mathrm{acc}}) = \frac{\alpha + (1-\alpha)\frac{\tau_{\mathrm{acc}}}{\tau_{\mathrm{m}}}}{\alpha + (1-\alpha)\frac{\tau_{\mathrm{acc}}}{\tau_{\mathrm{m}}}\frac{h_{\mathrm{acc}}}{h_{\mathrm{m}}}}h_{\mathrm{acc}}. \tag{10}$$

We show in Fig. 1 the mixed time-gap as a function of the penetration rate α for $\frac{\tau_{\mathrm{acc}}}{\tau_{\mathrm{m}}} = 0.1$, $h_{\mathrm{m}} = 1$, and four different values for the time-gap of ACC-equipped vehicles.

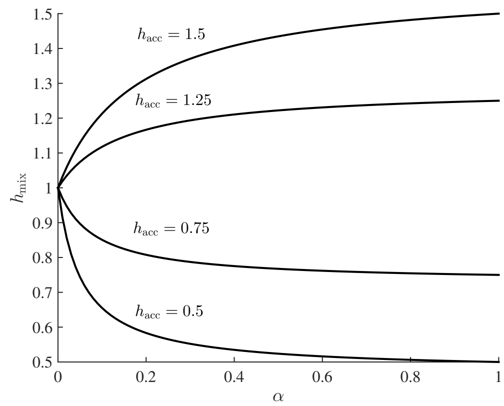

Fig. 1. Mixed time-gap (10) for $h_{\mathrm{m}} = 1$, $\frac{\tau_{\mathrm{acc}}}{\tau_{\mathrm{m}}} = 0.1$, and four different values of h_{acc}, as a function of the penetration rate α.

In the present work, we restrict our attention to congested regime, and thus, it is sufficient to define only the right part (i.e., for $\frac{1}{L} > \rho > \rho_{\min}$) of fundamental diagrams (6), (7). However, one may utilize any appropriate extension for the left part (i.e., for $0 < \rho \le \rho_{\min}$), such as, for example, a fundamental diagram that corresponds to a constant (free-flow) speed. We show in Fig. 2 an example of potentially meaningful fundamental diagrams (6) for different (but fixed) values of h_{acc}. Specifically, $Q_{h_{\min}}$ is fundamental diagram that corresponds to some minimum possible time-gap, say $h_{\min}$, which is related to $\rho_{\min}$ via $h_{\min} = \frac{\frac{1}{\rho_{\min}} - L}{v_{\mathrm{f}}}$, defined as [1]

$$Q_{h_{\min}}(\rho) = \begin{cases} v_{\mathrm{f}}\rho, & 0 \le \rho \le \rho_{\min} \\ \frac{1}{h_{\min}}(1 - L\rho), & \rho_{\min} < \rho \le \frac{1}{L} \end{cases}. \tag{11}$$

The fundamental diagram that corresponds to some maximum possible time-gap, say $h_{\max}$, is defined respectively as $Q_{h_{\max}}(\rho) = v_{\mathrm{f}}\rho$ for $0 \le \rho \le \bar{\rho}_{\min}$ and $Q_{h_{\max}}(\rho) = \frac{1}{h_{\max}}(1 - L\rho)$

[1] Although $Q_{h_{\min}}$ is not differentiable at $\rho_{\min}$, one could obtain a differentiable approximation of the original fundamental diagram.

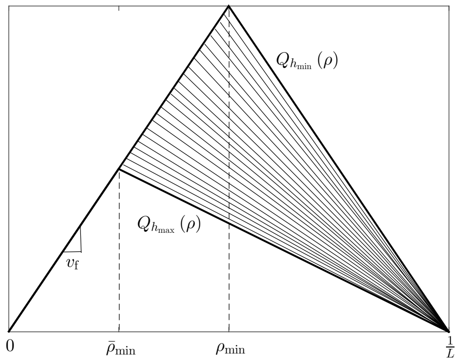

Fig. 2. Different fundamental diagrams (6) for $h_{\mathrm{acc}} \in [h_{\min}, h_{\max}]$.

for $\bar{\rho}_{\min} < \rho \leq \frac{1}{L}$, where $h_{\max}$ satisfies $h_{\max} = \frac{\frac{1}{\bar{\rho}_{\min}} - L}{v_{\mathrm{f}}}$ (for further details on realistic values of $h_{\max}$ and $h_{\min}$ that may appear in practice see Section 5 as well as, e.g., Nowakowski et al. (2011), Spiliopoulou et al. (2018)). Every other fundamental diagram (6) that may appear, for different time-gaps of ACC-equipped vehicles within the interval $[h_{\min}, h_{\max}]$, lies between $Q_{h_{\max}}$ and $Q_{h_{\min}}$. Furthermore, for a given penetration rate, since relation (10) implies that $\min\{h_{\mathrm{acc}}, h_{\mathrm{m}}\} \leq h_{\mathrm{mix}} \leq \max\{h_{\mathrm{acc}}, h_{\mathrm{m}}\}$, for all $\alpha \in [0,1]$, it follows that whenever $\min\{h_{\mathrm{acc}}, h_{\mathrm{m}}\} \geq h_{\min}$ and $\max\{h_{\mathrm{acc}}, h_{\mathrm{m}}\} \leq h_{\max}$, all of the possible mixed fundamental diagram relations (9) that may appear, for any $\alpha \in [0,1]$, lie between $Q_{h_{\max}}$ and $Q_{h_{\min}}$, and hence, as long as $\rho > \rho_{\min} = \frac{1}{L + v_{\mathrm{f}} h_{\min}}$ the mixed fundamental diagram relation (9) corresponds to congested traffic.

In addition, from (8) it follows that $\min\{\tau_{\mathrm{acc}}, \tau_{\mathrm{m}}\} \leq \tau_{\mathrm{mix}} \leq \max\{\tau_{\mathrm{acc}}, \tau_{\mathrm{m}}\}$, for all $\alpha \in [0,1]$, and hence, when $\tau_{\mathrm{acc}} < \tau_{\mathrm{m}}$, which is typically the case in practice, τ_{mix} is a decreasing function of α. Since for given values of v_{f} (dependent, for example, on the specific freeway stretch) and L, the requirements $\min\{h_{\mathrm{acc}}, h_{\mathrm{m}}\} \geq h_{\min}$ and $\max\{h_{\mathrm{acc}}, h_{\mathrm{m}}\} \leq h_{\max}$ guarantee that $0 < V_{\mathrm{mix}}(\rho, h_{\mathrm{acc}}) < v_{\mathrm{f}}$, for all $\alpha \in [0,1]$ and $\rho_{\min} < \rho < \frac{1}{L}$, we obtain a speed equation that may serve as a reasonable model for speed in case of mixed traffic in congested conditions.

Since we are concerned with the case of congested traffic conditions we restrict our attention in a nonempty, connected open subset Ω of the set $\bar{\Omega} = \Big\{(v, \rho, h_{\mathrm{acc}}) \in \mathbb{R}^3 : 0 < v < v_{\mathrm{f}}, \frac{1}{L + v_{\mathrm{f}} h_{\min}} < \rho < \frac{1}{L},\ h_{\min} \leq h_{\mathrm{acc}} \leq h_{\max}\Big\}$, such that $v + \rho \frac{\partial V_{\mathrm{mix}}(\rho, h_{\mathrm{acc}})}{\partial \rho} < 0$, for all $\alpha \in [0,1]$, whenever $(v, \rho, h_{\mathrm{acc}}) \in \Omega$, see, e.g., Belletti et al. (2015), Treiber & Kesting (2013). In fact, from (9), it is evident that (1)–(4) is a 2×2 system of first-order hyperbolic PDEs with (real and distinct) eigenvalues given by $\lambda_1 = v$ and $\lambda_2 = v + \rho \frac{\partial V_{\mathrm{mix}}(\rho, h_{\mathrm{acc}})}{\partial \rho} = v - \frac{1}{h_{\mathrm{mix}}(h_{\mathrm{acc}})\rho}$, which implies that information propagates forward with traffic flow at the traffic speed, whereas speed information travels backward. Thus, model (1)–(4) is anisotropic, see, e.g., Zhang (2002).

2.3 Boundary conditions of the system

The boundary condition (3) at the inlet of the considered freeway stretch implies that the flow at the entrance of the freeway stretch is equal to some external inflow with value q_{in}. To obtain a realistic downstream boundary condition as well as to obtain a well-posed system we impose the dynamic boundary condition (4), which implies free downstream traffic conditions, see also, e.g., Karafyllis et al. (2018). This is reasonable, even under congested conditions (consider, e.g., the case where at the outlet of the considered stretch there is the end of a tunnel or the end of high-curvature or the end of an upgrade, etc.).

2.4 Equilibria of the system

The equilibria of (1)–(4) dictated by constant inflow q_{in} and constant, steady-state time-gap for ACC-equipped vehicles, say $\bar{h}_{\mathrm{acc}}$, which results in a steady-state mixed time-gap given by

$$\bar{h}_{\mathrm{mix}} = \frac{\alpha + (1-\alpha)\frac{\tau_{\mathrm{acc}}}{\tau_{\mathrm{m}}}}{\alpha + (1-\alpha)\frac{\tau_{\mathrm{acc}}}{\tau_{\mathrm{m}}}\frac{\bar{h}_{\mathrm{acc}}}{h_{\mathrm{m}}}} \bar{h}_{\mathrm{acc}}, \tag{12}$$

are uniform and satisfy

$$\bar{v} = \frac{q_{\mathrm{in}}}{\bar{\rho}}, \tag{13}$$

as well as the fundamental diagram relation

$$\frac{1}{\bar{\rho}} - L = \bar{h}_{\mathrm{mix}} \bar{v}. \tag{14}$$

To see this, first note that relations (1) and (3) imply that the equilibrium values for ρ and v, say ρ^{e} and v^{e}, respectively, satisfy $\rho^{\mathrm{e}}(x) v^{\mathrm{e}}(x) = q_{\mathrm{in}}$, for all $x \in [0, D]$. From (2) and (4) it then follows, using (9), that the equilibrium profile of the speed satisfies the following ODE in x

$$v^{\mathrm{e}\prime}(x) = -\frac{1}{\tau_{\mathrm{mix}}} \frac{v^{\mathrm{e}}(x) + \frac{L}{\bar{h}_{\mathrm{mix}} - \frac{1}{q_{\mathrm{in}}}}}{v^{\mathrm{e}}(x)}, \tag{15}$$

with final condition $v^{\mathrm{e}}(D) = -\frac{L}{\bar{h}_{\mathrm{mix}} - \frac{1}{q_{\mathrm{in}}}}$. Thus,

$$v^{\mathrm{e}}(x) = \frac{L}{\frac{1}{q_{\mathrm{in}}} - \bar{h}_{\mathrm{mix}}} = \bar{v}, \quad \text{for all } x \in [0, D], \tag{16}$$

which can be seen noting that $v^{\mathrm{e}} = \bar{v}$ is an equilibrium of (15). In order to guarantee that $\rho_{\min} < \bar{\rho} < \frac{1}{L}$, $\forall \alpha \in [0,1]$, which also implies from (13), (14) that $0 < \bar{v} < \frac{1}{\bar{h}_{\mathrm{mix}}}\left(\frac{1}{\rho_{\min}} - L\right) \leq v_{\mathrm{f}}$, we require time-gaps and inflow to satisfy $0 < q_{\mathrm{in}} < \frac{v_{\mathrm{f}} h_{\min}}{h_{\max}(L + v_{\mathrm{f}} h_{\min})}$.

3. CONTROL DESIGN FOR THE LINEARIZED SYSTEM

3.1 Linearization and diagonalization of the system

We start defining the error variables $\tilde{\rho}(x,t) = \rho(x,t) - \bar{\rho}$, $\tilde{v}(x,t) = v(x,t) - \bar{v}$, and $\tilde{h}_{\mathrm{acc}}(x,t) = h_{\mathrm{acc}}(x,t) - \bar{h}_{\mathrm{acc}}$. Linearizing system (1)–(4) around the uniform, congested equilibrium profile we get

$$\tilde{\rho}_t(x,t) + \bar{v}\tilde{\rho}_x(x,t) + \bar{\rho}\tilde{v}_x(x,t) = 0 \tag{17}$$

$$\tilde{v}_t(x,t) - c_4 \tilde{v}_x(x,t) = -c_1 \tilde{\rho}(x,t) - c_2 \tilde{v}(x,t) - c_3 \tilde{h}_{\mathrm{acc}}(x,t) \tag{18}$$

$$\tilde{\rho}(0,t) + c_5 \tilde{v}(0,t) = 0 \tag{19}$$

$$\tilde{v}_t(D,t) = -c_1 \tilde{\rho}(D,t) - c_2 \tilde{v}(D,t) - c_3 \tilde{h}_{\mathrm{acc}}(D,t), \tag{20}$$

where $c_1 = \frac{1}{\bar{\rho}^2 \tau_{\mathrm{mix}} \bar{h}_{\mathrm{mix}}}$, $c_2 = \frac{1}{\tau_{\mathrm{mix}}}$, $c_3 = \frac{\alpha}{\tau_{\mathrm{acc}} \bar{h}_{\mathrm{acc}}^2} \left(\frac{1}{\bar{\rho}} - L \right)$, $c_4 = \frac{L}{\bar{h}_{\mathrm{mix}}}$, and $c_5 = \frac{\bar{\rho}}{\bar{v}}$. Defining $\tilde{z}(x) = e^{\frac{c_2 x}{\bar{v}}} \left(\tilde{\rho}(x) + \bar{h}_{\mathrm{mix}} \bar{\rho}^2 \tilde{v}(x) \right)$, as $c_2 - c_1 \bar{h}_{\mathrm{mix}} \bar{\rho}^2 = 0$, we re-write (17)–(20) in diagonal form as

$$\tilde{z}_t(x,t) + \bar{v} \tilde{z}_x(x,t) = -e^{\frac{c_2 x}{\bar{v}}} \bar{h}_{\mathrm{mix}} \bar{\rho}^2 c_3 \tilde{h}_{\mathrm{acc}}(x,t) \tag{21}$$

$$\tilde{v}_t(x,t) - c_4 \tilde{v}_x(x,t) = -c_1 e^{-\frac{c_2 x}{\bar{v}}} \tilde{z}(x,t) - c_3 \tilde{h}_{\mathrm{acc}}(x,t) \tag{22}$$

$$\tilde{z}(0,t) = -L \frac{\bar{\rho}^2}{\bar{v}} \tilde{v}(0,t) \tag{23}$$

$$\tilde{v}_t(D,t) = -c_1 e^{-\frac{c_2}{\bar{v}} D} \tilde{z}(D,t) - c_3 \tilde{h}_{\mathrm{acc}}(D,t). \tag{24}$$

3.2 Control law

Besides improving performance, feedback control is needed because (21)–(24) for $h_{\mathrm{acc}} = \bar{h}_{\mathrm{acc}}$ is unstable, see Bekiaris-Liberis & Delis (2018) (Appendix A). The control law is

$$h_{\mathrm{acc}}(x,t) = \bar{h}_{\mathrm{acc}} + \frac{1}{c_3} \left(-c_1 e^{-\frac{c_2 x}{\bar{v}}} \tilde{z}(x,t) + k \tilde{v}(x,t) \right) \tag{25}$$

$$= \bar{h}_{\mathrm{acc}} + \frac{1}{c_3} \left(-c_1 \tilde{\rho}(x,t) + (k - c_2) \tilde{v}(x,t) \right), \tag{26}$$

with $k > 0$ being arbitrary, which gives $\tilde{z}_t(x,t) + \bar{v} \tilde{z}_x(x,t) = c_2 \tilde{z}(x,t) - k e^{\frac{c_2 x}{\bar{v}}} \bar{h}_{\mathrm{mix}} \bar{\rho}^2 \tilde{v}(x,t)$, $\tilde{v}_t(x,t) - c_4 \tilde{v}_x(x,t) = -k \tilde{v}(x,t)$, $\tilde{z}(0,t) = -L \frac{\bar{\rho}^2}{\bar{v}} \tilde{v}(0,t)$, and $\tilde{v}_t(D,t) = -k \tilde{v}(D,t)$. From this system it is evident that the feedback law aims at eliminating the source term in (22), which may cause instability due to a feedback connection between the states $\tilde{z}$ and $\tilde{v}$, while rendering the $\tilde{v}(D)$ subsystem exponentially stable (and autonomous).

Taking into account that the traffic system operates in congested regime, the operating point of the controller, as this is seen via the steady-state time-gap for ACC-equipped vehicles $\bar{h}_{\mathrm{acc}}$, may vary considering, for example, safety, comfort, or total travel time criteria. For instance, in cases in which safety is a primary goal, the time-gap $\bar{h}_{\mathrm{acc}}$ may take large values (which implies that $\bar{h}_{\mathrm{mix}}$ also takes large values, according to (12)), whereas, when comfort is of significant importance, then no action (e.g., as recommendation to drivers of ACC-equipped vehicles or as direct manipulation of the ACC settings of individual vehicles) may be taken (in order to not disrupt the driver) from the controller for imposing the value of $\bar{h}_{\mathrm{acc}}$, which implies that the driver alone may set the value for the time-gap $\bar{h}_{\mathrm{acc}}$, see, e.g., Spiliopoulou et al. (2018). Moreover, it may be beneficial, from a total travel time point of view, the time-gap $\bar{h}_{\mathrm{acc}}$ to take large values, since, for given inflow, lower steady-state densities may be achieved (via the achievement of higher steady-state speeds), as it can be seen from relations (13), (16). We consider a specific scenario and further discuss about the choice of $\bar{h}_{\mathrm{acc}}$ (as well as of h_{m}) in Section 5.

In practice, under a vehicle-to-infrastructure (V2I) communication paradigm, the control authority may implement the proposed strategy either as time-gap recommendations to drivers of ACC-equipped vehicles or via direct manipulation of the ACC settings of such vehicles, see, e.g., Spiliopoulou et al. (2018). Furthermore, the simple controller (26), requires measurements of average speed and density (or, average speed and flow, in case flow measurements are available instead) throughout the spatial domain. This information could be obtained by the central control authority via utilization of connected vehicles (i.e., ACC-equipped and any vehicle able to exchange information with the central monitoring and control unit) reports (e.g., reporting speed, position, or other information) as well as measurements from fixed detectors and, potentially, also employing a traffic state estimation method, see, e.g., Bekiaris-Liberis et al. (2017), Claudel & Bayen (2010), Wang et al. (2017).

4. STABILITY ANALYSIS

We establish stability in the stronger C^1 norm in order to guarantee additional stability properties for the closed-loop system that may be desirable from a traffic flow control viewpoint, see, e.g., Yi & Horowitz (2006). Stability in other norms may be also proved, following the lines of the following theorem's proof, provided in Bekiaris-Liberis & Delis (2018) (Appendix B).

Theorem 1. Consider a closed-loop system consisting of system (17)–(20) and control law (26). For all initial conditions $(\tilde{\rho}(\cdot,0), \tilde{v}(\cdot,0)) \in C^1[0,D] \times C^1[0,D]$, which satisfy first-order compatibility with boundary conditions, there exists a positive constant μ such that the following holds for all $t \geq 0$

$$\|\tilde{\rho}(t)\|_{C^1} + \|\tilde{v}(t)\|_{C^1} \leq \mu \left(\|\tilde{\rho}(0)\|_{C^1} + \|\tilde{v}(0)\|_{C^1} \right) e^{-\frac{k}{2} t}. \tag{27}$$

5. SIMULATION RESULTS

5.1 Model parameters and numerical implementation

The parameters of system (1)–(4) utilized in the simulation investigations are shown in Table 1. The chosen parameters are

Table 1. Parameters of system (1)–(4).

q_{in}	$1200 \left(\frac{\mathrm{veh}}{\mathrm{h}}\right)$	τ_{acc}	2 (s)	h_{m}	1 (s)
ρ_{min}	$37 \left(\frac{\mathrm{veh}}{\mathrm{km}}\right)$	α	0.15	D	1000 (m)
τ_{m}	60 (s)	L	5 (m)		

considered reasonable for a traffic flow model, see, e.g., Belletti et al. (2015), Delis et al. (2015), Fan et al. (2014), Ngoduy (2013). In particular, we choose a value for the time-gap of manually driven vehicles h_{m} that is close to reported average values of about 1.2 s, see, e.g., Nowakowski et al. (2011), Spiliopoulou et al. (2018), but slightly lower than this to reflect evidence that drivers may follow a preceding vehicle at smaller time-gaps in congested traffic, compared to the case of light traffic conditions, see, e.g., Nowakowski et al. (2011).

For the numerical solution of the hyperbolic system (1)–(4) in open-loop as well as under (26), a modified Rusanov scheme, which is an explicit finite-volume scheme of centered type with added numerical diffusion, with time and spatial discretization steps of 0.1 s and 10 m, respectively, is employed, see, e.g., Dolejsi & Gallouet (2008). The ODE (4) that corresponds to the downstream boundary condition for the speed is numerically solved utilizing a forward Euler method with the same time step. The upstream and downstream boundary values for density and speed, respectively, are obtained from the boundary conditions (3) and (4), whereas for obtaining the "missing" upstream and downstream boundary values for speed and density, respectively, we use fictitious cells, extrapolating the corresponding values from the interior of the domain.

5.2 Controller's parameters and performance evaluation

The operating point of the traffic system, as it is dictated by the steady-state value of the mixed time-gap according to (12), it is selected such that $\bar{h}_{\text{acc}} = 1.5$ s. Such a value reflects the fact that the equilibrium of the time-gap for ACC-equipped vehicles may be dictated from drivers' choices rather than from interventions of the control authority, for a control strategy that aims at minimizing controller's interventions, which may be disrupting for the driver. Consequently, we choose a value for $\bar{h}_{\text{acc}}$ close to what drivers of ACC-equipped vehicles set in congested conditions, which is evidenced to be larger compared to manual driving in heavy traffic and which is reported to be around the selected value, see, e.g., Nowakowski et al. (2011).

The steady-state values for density and speed are derived from (13), (14) as $\bar{\rho}=105.8\ \frac{\text{veh}}{\text{km}}$, $\bar{v}=11.35\ \frac{\text{km}}{\text{h}}$. We show in Fig. 3 the open-loop response for initial conditions $\rho(x,0) = \bar{\rho} + 10\cos\left(\frac{8\pi x}{D}\right)$, $v(x,0)=\frac{q_{\text{in}}}{\rho(x,0)}$. From Fig. 3 it is evident that the open-loop response exhibits an unstable and quite oscillatory behavior. In contrast, as it is shown in Fig. 4, the traffic flow is stabilized and, in particular, the oscillations (stop-and-go waves) in the speed response are considerably suppressed when the feedback law (26) is applied. The control effort (26) for $k = 0.25\ \frac{1}{\text{s}}$ is shown in Fig. 5. One can observe that the resulting values for the time-gap of ACC-equipped vehicles lie within the bounds typically implemented in ACC-equipped vehicles settings, namely, approximately within the interval $[0.8, 2.2]$ s, see, e.g., Nowakowski et al. (2011), Spiliopoulou et al. (2018).

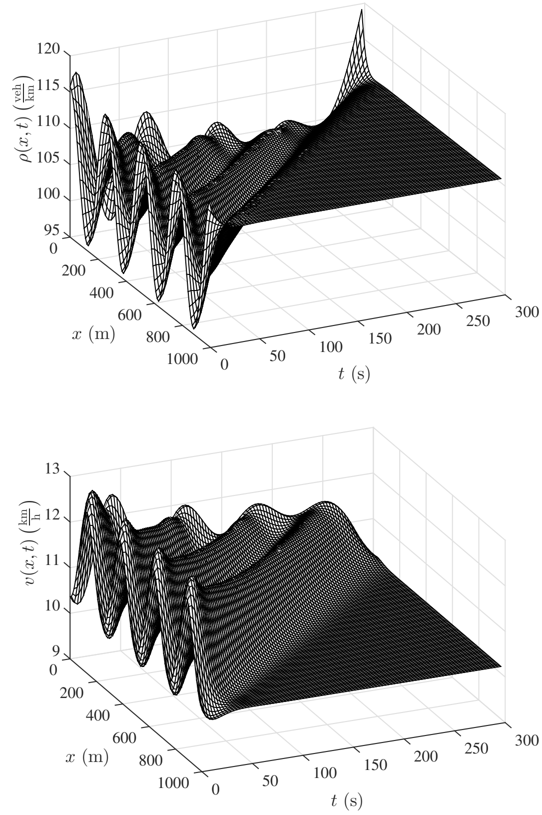

Fig. 3. Open-loop response of (1)–(4) with parameters in Table 1 for $\bar{h}_{\text{acc}}$=1.5, $\rho(x,0)$=$\bar{\rho}$+$10\cos\left(\frac{8\pi x}{D}\right)$, $v(x,0)$=$\frac{q_{\text{in}}}{\rho(x,0)}$.

To quantify the benefits of controller (26) we compare the closed- and open-loop performances in terms of fuel consumption, comfort, and total travel time (TTT). We use the performance indices from Treiber & Kesting (2013) (Chapter 21) $J_{\text{fuel}} = \int_0^T \int_0^D \bar{J}_{\text{fuel}}\left(v(x,t), a(x,t)\right)\rho(x,t)dxdt$, $J_{\text{comfort}} = \int_0^T \int_0^D$

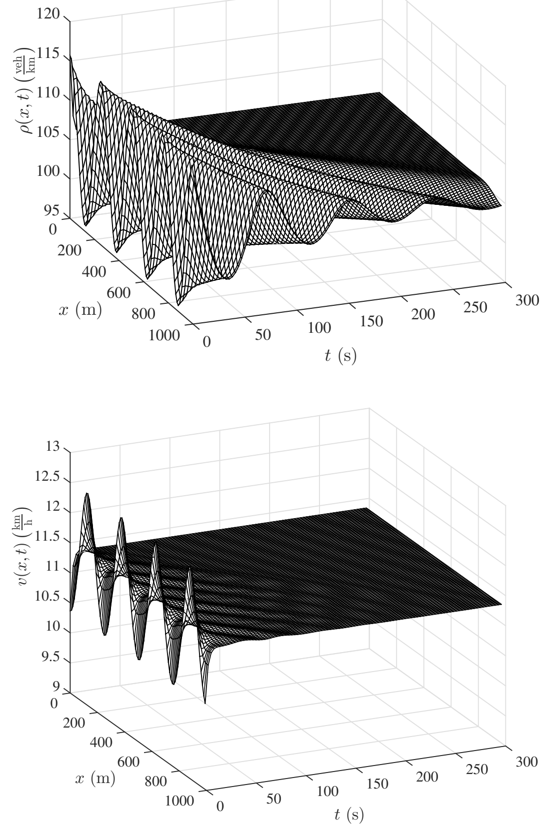

Fig. 4. Closed-loop response of (1)–(4) with parameters in Table 1, under the feedback law (26) with $k = 0.25$, for $\bar{h}_{\text{acc}} = 1.5$ and $\rho(x,0) = \bar{\rho} + 10\cos\left(\frac{8\pi x}{D}\right)$, $v(x,0) = \frac{q_{\text{in}}}{\rho(x,0)}$.

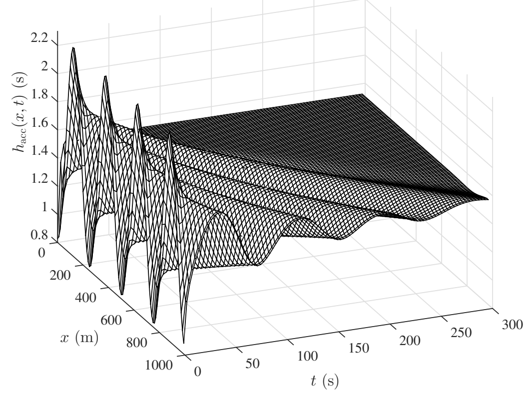

Fig. 5. Feedback control law (26) with $k = 0.25$ and $\bar{h}_{\text{acc}} = 1.5$.

$\left(a(x,t)^2 + a_t(x,t)^2\right)\rho(x,t)dxdt$, and $J_{\text{TTT}} = \int_0^T \int_0^D \rho(x,t)dxdt$, where $\bar{J}_{\text{fuel}}(v,a) = \max\left\{0, b_0 + b_1 v + b_3 v^3 + b_4 va\right\}$, $a = v_t + vv_x$, $T = 350$ s, and b_0, b_1, b_3, b_4 are provided in Treiber & Kesting (2013) (page 485). Application of the controller results in better performance in all metrics. Specifically, the reported percentage improvement of J_{fuel}, J_{comfort}, and J_{TTT} is 3.9%, 90%, and 4%, respectively. The improvement in fuel consumption and comfort is attributed to the fast homogenization of the speed field.

6. CONCLUSIONS

We presented a control design methodology for stabilization of traffic flow in congested regime exploiting the capabilities of vehicles with ACC features and utilizing an ARZ-type model for mixed traffic. The closed-loop system, under the developed control law, was shown to be exponentially stable. The numerical investigation showed that the performance of the considered traffic system, under the proposed controller, is improved and the improvement, in terms of fuel consumption, travel time, and comfort, was quantified utilizing various performance indices.

ACKNOWLEDGMENTS

Nikolaos Bekiaris-Liberis was supported by the funding from the European Commission's Horizon 2020 research and innovation programme under the Marie Sklodowska-Curie grant agreement No. 747898, project PADECOT.

The authors thank Dr. Diamantis Manolis, Prof. Markos Papageorgiou, and Prof. Claudio Roncoli for fruitful discussions.

REFERENCES

G. Bastin & J.-M. Coron. *Stability and Boundary Stabilization of 1-D Hyperbolic Systems*. Birkhauser, Basel, 2016.

N. Bekiaris-Liberis and A. M. Bayen. Nonlinear stabilization of a viscous Hamilton-Jacobi PDE. *IEEE Transactions on Automatic Control*, 60: 1698–1703, 2014.

N. Bekiaris-Liberis & A. Delis. PDE-based feedback control of freeway traffic flow via time-gap manipulation of ACC-equipped vehicles. *arXiv*, 1812.08154, 2018.

N. Bekiaris-Liberis, C. Roncoli, and M. Papageorgiou. Highway traffic state estimation per lane in the presence of connected vehicles. *Transp. Res. B*, 106: 1–28, 2017.

F. Belletti, M. Huo, X. Litrico, & A. M. Bayen. Prediction of traffic convective instability with spectral analysis of the Aw-Rascle-Zhang model. *Physics Let. A*, 379: 2319–2330, 2015.

S. Blandin, X. Litrico, B. Piccoli, & A. Bayen. Regularity and Lyapunov stabilization of weak entropy solutions to scalar conservation laws. *IEEE Trans. on Automatic Control*, 62: 1620–1635, 2017.

A. Bose & P. Ioannou. Mixed manual/semi-automated traffic: a macroscopic analysis. *Transp. Res. C*, 11: 439–462, 2003.

C. Chen, Z. Jia, P. Varaiya. Causes and cures of highway congestion. *IEEE Cont. Sys. Mag.*, 21: 26–32, 2001.

C. Claudel & A. Bayen. Lax-Hopf based incorporation of internal boundary conditions into Hamilton-Jacobi equation–Part I: Theory. *IEEE Transactions on Automatic Control*, 55: 1142–1157, 2010.

A. I. Delis, I. K. Nikolos, M. Papageorgiou. Macroscopic traffic flow modelling with adaptive cruise control: Development and numerical solution. *Comp. & Mathem. with App.*, 70: 1921–1947, 2015.

M. L. Delle Monache, B. Piccoli, and F. Rossi. Traffic regulation via controlled speed limit. *SIAM Journal of Control and Optimization*, 55: 2936–2958, 2017.

C. Diakaki, M. Papageorgiou, I. Papamichail, & I. Nikolos. Overview and analysis of Vehicle Automation and Communication Systems from a motorway traffic management perspective. *Transp. Res. Part A*, 75: 147–165, 2015.

V. Dolejsi & T. Gallouet. A numerical study of a particular non-conservative hyperbolic problem. *Computers and Fluids*, 37: 1077–1091, 2008.

S. Fan, M. Herty, and B. Seibold. Comparative model accuracy of a data-fitted generalized Aw-Rascle-Zhang model. *Networks and Heterogeneous Media*, 9: 239–268, 2014.

P. Goatin, S. Gottlich & O. Kolb. Speed limit and ramp meter control for traffic flow networks. *Eng. Optim.*, 48: 1121–1144, 2016.

M. Herty, W.-A. Yong. Feedback boundary control of linear hyperbolic systems with relaxation. *Automatica*, 69: 12–17, 2016.

I. Karafyllis, N. Bekiaris-Liberis, and M. Papageorgiou. Feedback control of nonlinear hyperbolic PDE systems inspired by traffic flow models. *IEEE Transactions on Automatic Control*, in press, 2018.

A. M. Kesting, M. Treiber, M. Schonhof, & D. Helbing. Adaptive cruise control design for active congestion avoidance. *Transp. Res. Part C*, 16: 668–683, 2008.

P.-O. Lamare & N. Bekiaris-Liberis. Control of 2×2 linear hyperbolic systems: Backstepping-based trajectory generation and PI-based tracking. *Syst. & Control Let.*, 86: 24–33, 2015.

P. Y. Li, R. Horowitz, L. Alvarez, J. Frankel, A. M. Robertson. An automated highway system link layer controller for traffic flow stabilization. *Transp. Research Part C*, 5: 11–37, 1995.

D. Ngoduy. Instability of cooperative adaptive cruise control traffic flow: A macroscopic approach. *Commun. Nonlinear Sci. Numer. Simulat.*, 18: 2838–2851, 2013.

C. Nowakowski, S. E. Sladover, D. Cody, F. Bu, J. O'Connell, J. Spring, S. Dickey, D. Nelson. Cooperative adaptive cruise control: Testing drivers choices of following distances. *California PATH Res. Rep.*, 2011.

G. Piacentini, P. Goatin, & A. Ferrara. Traffic control via moving bottleneck of coordinated vehicles. *IFAC CTS Sym.*, Savona, Italy, 2018.

W. J. Schakel & B. van Arem. Improving traffic flow efficiency by in-car advice on lane, speed, and headway. *IEEE Trans. Intel. Transp. Systems*, 15: 1597–1606, 2014.

A. Spiliopoulou, D. Manolis, F. Vandorou, M. Papageorgiou. Adaptive cruise control operation for improved motorway traffic flow. *Transportation Research Record*, in press, 2018.

D. Swaroop & K. R. Rajagopal. Intelligent cruise control systems and traffic flow stability. *TR–Part C*, 7: 329–352, 1999.

M. Treiber & A. Kesting. *Traffic Flow Dynamics–Data, Models and Simulation*. Springer, Berlin, 2013.

Y. Yi & R. Horowitz. Macroscopic traffic flow propagation stability for adaptive cruise controlled vehicles. *Transportation Research Part C*, 14: 81–95, 2006.

R. Vazquez & M. Krstic. Marcum Q-functions and explicit kernels for stabilization of 2×2 linear hyperbolic systems with constant coefficients. *Sys. & Cont. Let.*, 68: 33–42, 2014.

R. Wang, Y. Li, & D. B. Work. Comparing traffic state estimators for mixed human and automated traffic flows. *Transportation Research Part C*, 78: 95–110, 2017.

H. Yu, S. Koga, & M. Krstic. Stabilization of traffic flow with autonomous vehicles. *ASME DSCC*, Atlanta, GA, 2018.

H. Yu & M. Krstic. Traffic congestion control for Aw-Rascle-Zhang model. *Automatica*, 100: 38–51, 2019.

H. M. Zhang. A non-equilibrium traffic model devoid of gas-like behavior. *Transp. Research Part B*, 36: 275–290, 2002.

L. Zhang & C. Prieur. Necessary and sufficient conditions on the exponential stability of positive hyperbolic systems. *IEEE Trans. Autom. Control*, 62: 3610–3617, 2017.

L. Zhang & C. Prieur. Stochastic stability of Markov jump hyperbolic systems with application to traffic flow control. *Automatica*, 86: 29–37, 2017.